Photoelectron Production and Transport in the Upper Atmosphere

Jhoon Kim

Space Division, Korea Aerospace Research Institute, 52 Eoun-dong, Yusong-gu,
Taejon 305-333, Korea

Abstract

Theory and observations relating to the photoelectrons are reviewed.
The photoelectrons play a very important role in the photochemistry and
energetics of the upper atmosphere. It is a dominant heating source for
the ambient electrons in the ionosphere. This paper covers the solar EUV
flux calculation, local photoelectron production rates and the two-stream
approximation of the photoelectron transport in the upper atmosphere.
Some data are compiled and tabulated for reference.

1. Introduction

The atmosphere of any planet exposed to the solar EUV radiation is photoionized to
produce free electrons and ions, forming and maintaining the ionosphere. These solar EUV
radiation is major cause of ionization in the lower ionosphere where the atmospheric
constituents are abundant. The photoelectrons produced in the photoionization process play
an important role in the upper atmosphere and are the most significant heat source to the
upper atmosphere. These electrons can lose its excess energy in the same region where they
were created, but can also travel to the other region in the atmosphere depending on their
energy. Thus it is necessary to consider the transport of photoelectrons as well as local

production. In this paper, these two important processes are reviewed with the method to calculate the solar flux for the period when one wishes to consider.

2. Solar Flux

Solar flux is the most important part for the photoelectron spectrum calculation and its photochemistry. The intensity of the EUV/UV radiation varies with the solar activity. The solar EUV intensities were taken from the reference values given by Hinteregger (1981a) and Hinteregger et al. (1981) and modified by Torr and Torr (1985). For the specific period of time, one needs to scale the solar flux appropriately with known parameters as in Table 1. Other important parameters and resulted solar fluxes for the solar maximum and minimum periods are tabulated and presented in Appendix. In the table, K=0 represents the case where the solar flux at the desired time periods can be calculated using the equation that will be described below with B parameter given in Table 1.

The reference spectrum were appropriately scaled for the solar maximum(1979-1980) and solar minimum(1984-1986) periods, using measured 10.7 cm flux values and scaling factors recommended by Hinteregger et al. (1981). He recommended that two classes of emissions should be considered: K=1 for which the key index is the emission at λ=102.6 nm (H Ly α) and K=2 for which the emission at λ=33.5 nm (Fe XVI) is used as the appropriate

Table 1. The B parameters associated with equation (1) for solar UV flux variation adjustments (taken from Kim, 1991).

λ (nm)	B_0	B_1	B_2
16.8-19.0	1.0	0.01122	0.00256
19.0-20.6	1.0	0.03123	0.00590
20.6-25.5	1.0	0.02391	0.0071
25.5-30.0	1.0	0.03830	0.01259
30.4	1.0	0.00605	0.00325
51.0-58.0	1.0	0.00964	0.00255
58.4	1.0	0.01130	0.00438
59.0-60.6	1.0	0.01101	0.00244
102.6	1.0	0.01380	0.00500
33.5	1.0	0.59425	0.38110
121.6	1.0	0.01176	0.00306
28.4	1.0	0.22811	0.11638
20.0-20.4	1.0	0.04562	0.00918
17.8-18.3	1.0	0.01272	0.00290
16.9-17.3	1.0	0.00616	0.00178

index. Hinteregger (1981) suggested the following relationship for the ratio of the solar flux on a given day to that of the reference value:

$$\frac{I(\lambda)}{I_{ref}(\lambda)} \;=\; B_0 + B_1[\langle F_{10.7} \rangle_{81d} - 71.5] + B_2[F_{10.7} - \langle F_{10.7} \rangle_{81d} + 3.9], \tag{1}$$

where $F_{10.7}$ is the daily value of the 10.7-cm flux (10^{-22} W m^{-2} Hz^{-1}), $\langle F_{10.7} \rangle_{81d}$ is the 81-day average value of the 10.7-cm flux, and B_0, B_1, B_2 are the parameters given in Table 1. For an estimate of the solar flux over wavelength intervals not covered by the B parameters, one needs to estimate the two key wavelength intensities at $\lambda = 33.5$ nm and $\lambda = 102.6$ nm, using equation (1), and then use the following equation to scale the reference flux as necessary:

$$I(\lambda) \;=\; I_{ref}(\lambda)[1 + C_\lambda(R_K - 1)], \tag{2}$$

where R_K is the ratio of flux intensity at the desired time to that of the reference value ($\lambda = 33.5$ nm for K=1 and $\lambda = 102.6$ nm for K=2) and C_λ is the effective contrast ratio provided with the reference flux. The scaled solar flux for the two periods together with parameters and reference flux compiled from EUV spectrometer on Atmospheric Explorer (AE)-E are listed in Appendix.

Fig. 1(a) shows solar EUV fluxes in 25 Å intervals where the absolute values estimated were referred to January 22, 1979. The $F_{10.7}$ values was 234 and the 81-day average of $F_{10.7}$.
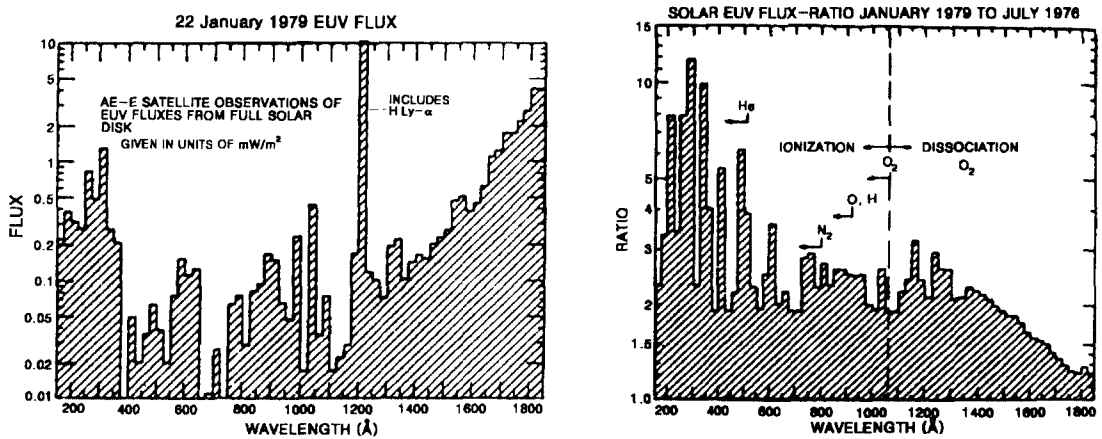

Fig. 1. (a) Solar EUV fluxes in 25 Å intervals where the absolute values estimated were referred to January 22, 1979 ($F_{10.7}$ = 234, $\langle F_{10.7} \rangle_{81d}$ = 198, A_p = 10). (b) The ratios of solar EUV fluxes in (a) to the averages of 24 sets of observations obtained during July 1976 on days with R_z = 0 and $F_{10.7}$ < 70 ($\langle F_{10.7} \rangle_{81d}$=71, A_p = 9).

$\langle F_{10.7}\rangle_{81d}$ was 198 and A_p index was 10. Fig. 1(b) shows the ratios of solar EUV fluxes in Fig. 1(a) to the averages of 24 sets of observations obtained during July 1976 on days with R_z = 0 and $F_{10.7}$ less than 70 ($\langle F_{10.7}\rangle_{81d}$=71 and A_p = 9). Fig. 2 shows the monthly mean values of solar irradiance for three different EUV fluxes of H Ly-α, H Ly-β, and He I 584 Å The solid circles were calculated as 31-day mean values centered on the middle of the month of all existing AE-E observations. One should note the good correlation of the $F_{10.7}$ values to the shown solar EUV fluxes.

3. Photoelectron Production

When the solar EUV radiation ionizes the atmospheric constituents in the lower ionosphere, it produces electron. The electron produced in this process is called as photoelectron. The initial spectrum of photoelectrons generally reflects the features of the spectral distribution of solar photons, but is distorted locally as a result of the many different ionization energies for the atmospheric gases. A plot of the initial energy spectra of
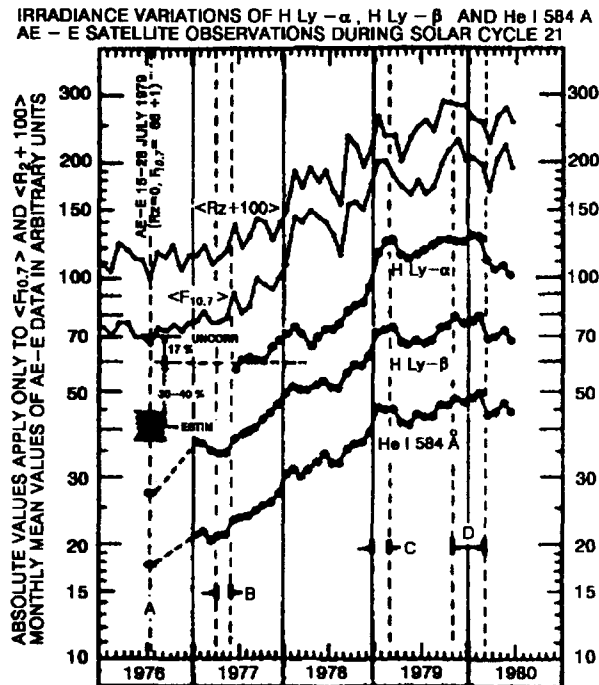

Fig. 2. Monthly mean values of solar irradiance for three different EUV fluxes. The solid circles represent the calculated 31-day mean values of all existing AE-E observations. The average $F_{10.7}$ values are shown together for comparison.
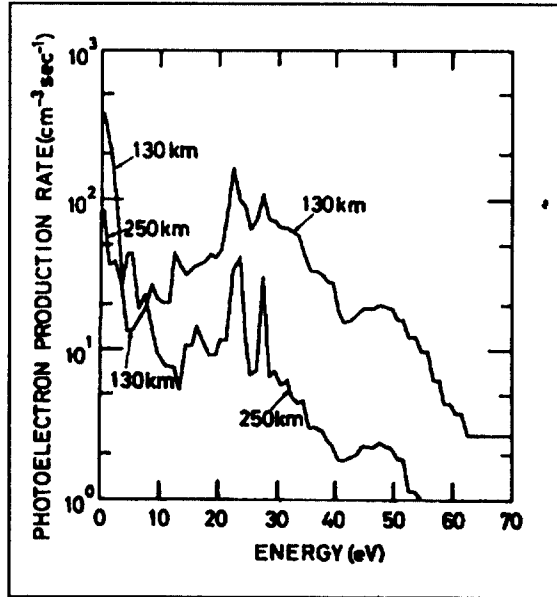
Fig. 3. Initial energy spectrum of photoelectrons at
two altitudes for an overhead sun and 1250
^{0}K thermosphere. The strong peaks between
20 and 30 eV arise from He(II)(304) (Nagy
and Banks, 1970).

photoelectron at different altitudes for an overhead sun is given in Figure 3. For example, the
atomic oxygen is photoionized by the solar EUV radiation to form a pair of electron and ion:

$$O + h\nu (E > 13.62 \text{ eV or } \lambda < 91.03 \text{ nm}) \rightarrow O^+ + e. \qquad (R1)$$
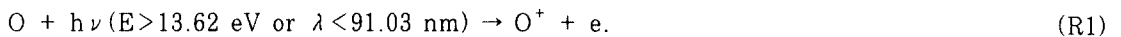
The absorption of radiation with wavelengths λ less than 91.03 nm (or E = 13.62 eV)
(which is called as ionization threshold potential) results in the ionization of atomic oxygen.
The ionization peak occurs at about 150 km owing mainly to the absorption of radiation with
wavelengths less than 79.6 nm. The ionization threshold of the atmospheric species are
given in Table 2. The free electrons produced in this photoionization process are called as
'photoelectron' which carries the excess energy of the photoionization. Photoelectrons are the
major heating source for ambient electrons in the ionosphere.

If the photoelectron produced as a result of photoionization has enough energy to ionize
the other atmospheric constituents, say atomic oxygen, then it can ionize other constituents
by collision. For example, if the atomic oxygen absorbs the solar EUV radiation at 41.3 nm
or with 30 eV energy,

$$O + h\nu (E = 30 \text{ eV or } \lambda = 41.3 \text{ nm}) \rightarrow O^+ + e^{*}(E = 30 - 13.62 \text{ eV}). \qquad (R1)$$
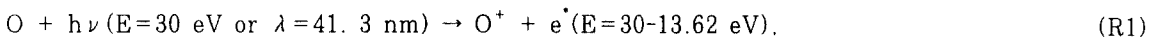
the photoelectron produced in photoionization can collide with other atomic oxygen

Table 2. Ionization threshold potentials

Neutral constituent	Ionization potential	
	(eV)	(nm)
C	11.26	110.1
CH_4	12.55	98.79
CO	14.01	88.49
CO_2	13.77	90.04
H	13.6	91.16
H_2	15.43	80.35
H_2O	12.62	98.24
He	24.59	50.42
Mg	7.46	162.2
N	14.53	85.33
N_2	15.58	79.58
NH_3	10.17	121.9
NO	9.264	133.8
Na	5.139	241.3
O	13.62	91.03
O_2	12.06	102.8
OH	13.18	94.07
S	10.36	119.7

$$O + e^{\cdot}(E=26.38 \text{ eV}) \rightarrow O^+ + e + e^{\cdot}(E=26.38-13.62 \text{ eV}), \qquad (R2)$$
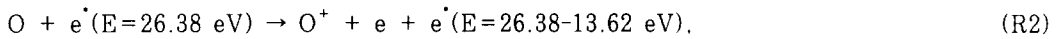
producing another electron-ion pair. This process is called as secondary ionization or electron impact ionization. There are other important photoionization in the E and F region of the ionosphere:

$$N_2 + h\nu \rightarrow N_2^+ + e, \qquad (R3)$$

$$\rightarrow N^+ + N + e, \qquad (R4)$$

$$O_2 + h\nu \rightarrow O_2^+ + e, \qquad (R5)$$

The photoelectron production rate is given by

$$P_e^{'}(E, z) = \sum_i \sum_n n_n(z) \int_0^\infty d\lambda I_\infty(\lambda) \sigma_n^{(i)}(\lambda) \, p_n(\lambda, E_i) \cdot \exp[-\tau(\lambda, z)], \qquad (3)$$

where τ is the optical depth given by

$$\tau(\lambda, z) = \sum_n \sigma_n^{(a)}(\lambda) \int_z^\infty N_n(z')dz' = \sum \sigma_n^{(a)}(\lambda) n_n H_n ch(R_{n}, \chi), \qquad (4)$$

H_n is the scale height of the atmospheric constituent n, given by

$$H_n = \frac{kT_n}{m_n g},$$ (5)

$R_n = (R+z)/H_n$, $E = E_\lambda - E_\iota$, E_λ is the corresponding energy to wavelength λ, E_ι is the ionization energy of a given excited ion state ι, R is the planetary radius. χ is the solar zenith angle. $ch(R_n, \chi)$ is the Chapman function(Chapman, 1931), n_n is the number density of atmospheric constituents. $I_\infty(\lambda)$ is the solar radiation spectrum at the top of the atmosphere, $\sigma_n^{(a)}(\lambda)$ is the absorption cross section of species n at wavelength λ, $\sigma_n^{(i)}(\lambda)$ is the ionization cross section, and $p_n(\lambda, E_\iota)$ is the branching ratios of various excited ion states.

The calculated photoelectron energy spectra are shown in Fig. 4(a) Photoelectrons with energies less than several electron volts tend to lose their energy by elastic collisions to ambient electrons rather than ions or neutral particles. On the other hand, if rapid inelastic processes such as rotational or vibrational excitation are involved, energy loss to neutrals can be more rapid. Measurements of photoelectron energy spectra have been made by sounding rockets and satellites for a different atmospheric conditions and shown in Fig. 4(b) Comparing Fig. 4(a) and 4(b) the calculated spectra shows more jagged behavior than that of measurement. In general, the calculation and measurement is in reasonable agreement.
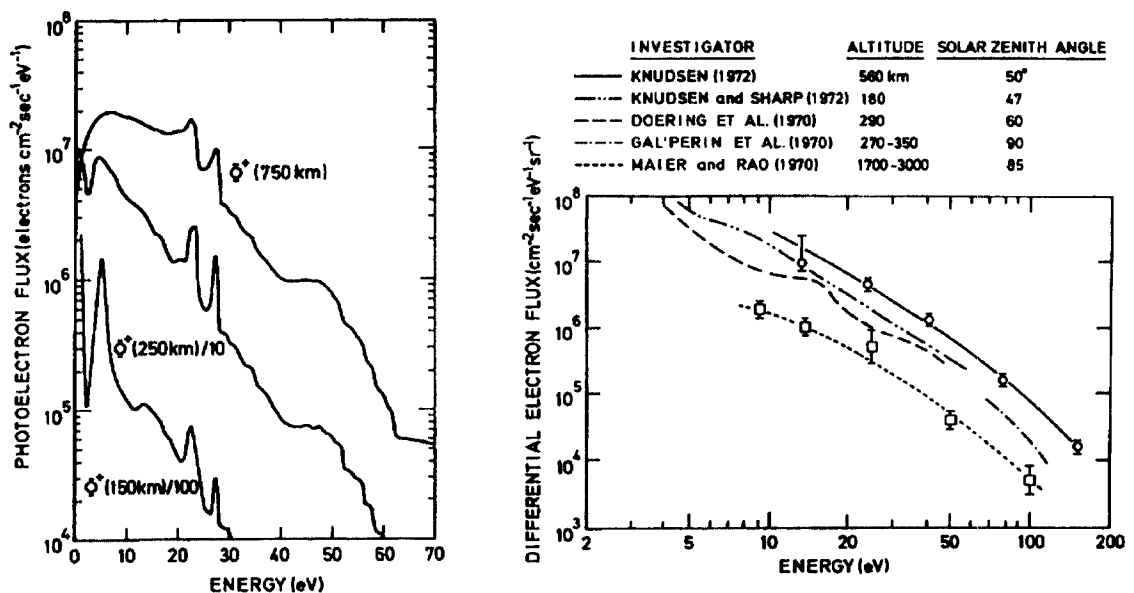

Fig. 4. (a) Calculated daytime photoelectron energy spectra at three altitudes for 750 ^{0}K thermosphere. (b)Experimental values for the differential photoelectron flux at various altitudes and solar zenith angles. (Banks and Kockarts, 1973)

4. Photoelectron Transport — Two Stream Approximation

Electron impact ionization is also important. especially in the lower ionosphere below the ionospheric peak. In calculating the impact ionization rates. particle transport. as well as elastic and inelastic processes must be taken into account. The photoelectron flux can be calculated by solving the widely-used two-stream equations for upward($\Phi+$) and downward ($\Phi-$) fluxes of photoelectrons in the energy range ε. $\varepsilon+d\varepsilon$ (Nagy and Banks. 1970) :

$$-\frac{\partial\Phi^+}{\partial s} = \frac{-1}{\langle\cos\theta\rangle}\sum_k n_k[\sigma_a^k+P_e^k\sigma_e^k]\,\Phi^+ + \frac{1}{\langle\cos\theta\rangle}\sum_k n_k p_e^k\sigma_e^k\,\Phi^- + \frac{1}{\langle\cos\theta\rangle}\left[\frac{q}{2}+q^+\right], \quad (6)$$

$$-\frac{\partial\Phi^-}{\partial s} = \frac{1}{\langle\cos\theta\rangle}\sum_k n_k[\sigma_a^k+P_e^k\sigma_e^k]\,\Phi^- - \frac{1}{\langle\cos\theta\rangle}\sum_k n_k p_e^k\sigma_e^k\,\Phi^+ + \frac{1}{\langle\cos\theta\rangle}\left[\frac{q}{2}+q^-\right], \quad (7)$$

where

z	the distance in vertical direction (positive upward).
$\Phi^+(\varepsilon,z)$	the photoelectron flux outward along z.
$\Phi^-(\varepsilon,z)$	the photoelectron flux inward along z.
$n_k(z)$	the k-th species number density.
$p_e^k(\varepsilon)$	the photoelectron backscatter probability for elastic collisions with the k th species.
$\sigma_e^k(\varepsilon)$	the photoelectron total scattering cross section for elastic collisions with the k th species.
$q(\varepsilon,z)$	the photoelectron production rate in the range ε to ε +d ε due to direct ionization processes.
$q\pm$	the photoelectron production in the range ε to ε +d ε due to cascading from higher energy photoelectrons undergoing inelastic collisions.
p_{aj}^k	the photoelectron backscatter probability for collisions with the k th species resulting in the j th inelastic process.
σ_{aj}^k	the inelastic cross section for the j th excitation of the k th particle species. and
$\langle\cos\theta\rangle$	the mean pitch angle for Φ^+ and Φ^- photoelectrons.

The first terms on the right hand sides of the two equations contribute the loss of upward and downward flux. respectively. All other terms on the right hand side contribute to the source of upward and downward flux. respectively. The calculations of the photoelectron fluxes by the above described two-stream method were made by Nagy and Banks (1970) and
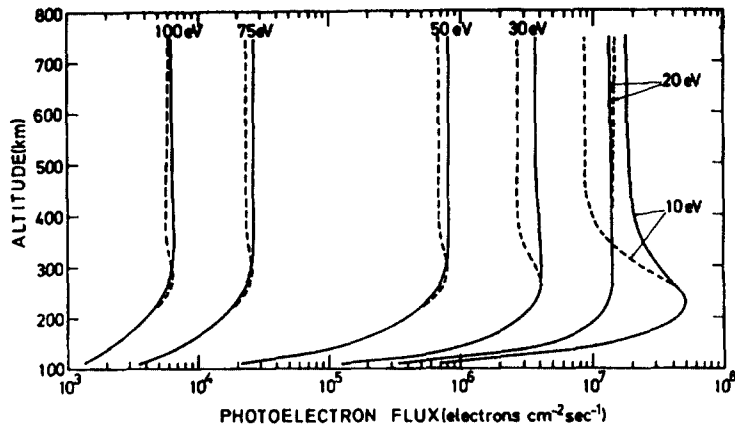
Fig. 5. Photoelectron fluxes for a sunlit 750 ^{0}K thermosphere and overhead sun. Solid and dashed curves represent the upward (Φ^+) and the downward flux (Φ^+), respectively.

are shown in Fig. 5. One can note that the difference between the upward and downward flux is larger at low energies, principally as a result of the strong photoelectron-thermal electron energy transfer rate.

5. Summary

The two important process of photoelectrons were reviewed together with the solar flux variation by $F_{10.7}$ index. Both the theoretical and experimental aspect of the photoelectron production and transport were described and compared. Photoelectrons which are mainly produced by the solar EUV radiation and transported by their own energy play a very important role in the photochemistry and energetics of the upper atmosphere.

References

Banks and Kockarts, *Aeronomy Vol. B*, Academic Press, 355 pp, 1973.

Hinteregger, H.E., Representations of solar EUV fluxes for aeronomical applications, *Adv. Space Res.*, *1*, 39, 1981a.

Hinteregger, H.E., Solar irradiance and its variations at wavelengths below 185 nanometer, Paper presented for the Middle Atmosphere Symposium at the IAGA, 1981b.

Hinteregger, H.E., Fukui, K., and Gilson, B.R., Observational reference and model data on solar EUV from measurements on AEE, *Geophys. Res. Lett.*, *8*, 1147, 1981.

Kim, J., Model studies of the ionosphere of Venus: ion composition, energetics and dynamics, *Ph.D. Thesis*, the University of Michigan, Ann Arbor, 1991.

Nagy and Banks. Photoelectron fluxes in the ionosphere. *J. Geophys. Res..* 75,6260. 1970.

Torr. M.R.. Torr. D.G.. Ong. R.A.. and Hinteregger. H.E.. Ionization frequencies for major thermospheric constituents as a function of solar cycle 21. *Geophys. Res. Lett., 6,* 771. 1979.

Torr. M.R.. and Torr. D.G.. Ionization frequencies for solar cycle 21: Revised. *J. Geophys. Res., 90.* 6675. 1985.

APPENDIX. Solar UV/EUV Flux Data for the
1979-1981 and 1984-1986 Periods (Kim, 1991)

Incident Solar UV/EUV flux Data (3-130.6 nm) for the solar maximum(1979-1981) and solar minimum(1984-1986) periods together with reference solar flux, K value and contrast ratio, C_λ.

λ (nm)	Reference Solar flux	K	C_λ	Solar flux solar max (10^9photons cm^{-2} s^{-1})	Solar flux solar min
130.600-130.490	0.0920	1	0.820009	0.2248	0.1057
130.220-130.220	1.1550	1	0.415009	1.9985	1.2422
126.500-126.500	0.2870	1	0.820009	0.7011	0.3298
126.070-126.070	0.1540	1	0.415009	0.2665	0.1656
124.280-124.280	0.0840	1	1.500000	0.3057	0.1069
123.880-123.880	0.1910	1	1.245009	0.6094	0.2343
121.570-121.570	300.0000	0*	R_K(x)=2.4949 R_K(n)=1.1500	748.4610	345.0000
120.650-120.650	4.2500	0*	R_K(x)=2.7597 R_K(n)=1.1800	11.7286	5.0150
117.500-117.500	2.7830	1	0.608009	5.7605	3.0910
112.830-112.830	0.3870	1	0.581009	0.7827	0.4279
112.250-112.250	0.3120	1	0.581009	0.6310	0.3450
108.500-108.500	0.0540	1	0.498009	0.1013	0.0589
103.760-103.760	0.9620	1	1.041009	2.7242	1.1443
103.190-103.190	1.9420	1	1.041009	5.4994	2.3099
131.000-128.000	3.7900	1	0.820009	9.2588	4.3556
128.000-125.000	2.3400	1	0.820009	5.7165	2.6892
125.000-122.000	0.5500	1	0.820009	1.3436	0.6321
113.000-110.000	0.0700	1	0.498009	0.1313	0.0763
110.000-107.000	2.2370	1	0.498009	4.1974	2.4398
107.000-104.000	0.9900	1	0.498009	1.8576	1.0797
104.000-102.700	0.7530	1	0.498009	1.4129	0.8212
102.580-102.570	4.3750	1	1.000009	12.0737	5.1712
101.030-101.010	0.0850	1	0.498009	0.1595	0.0927
99.160- 99.150	0.3830	1	0.523009	0.7355	0.4195
102.700- 99.000	0.5070	1	0.498009	0.9513	0.5530
97.710- 97.700	4.8480	1	0.498009	9.0965	5.2874
97.260- 97.250	0.7540	1	1.000009	2.0808	0.8912
99.000- 95.000	0.4660	1	0.498009	0.8744	0.5082
94.980- 94.970	0.3790	1	1.000009	1.0459	0.4480
94.460- 94.450	0.0770	1	0.498009	0.1445	0.0840
93.790- 93.770	0.2280	1	1.000009	0.6292	0.2695
93.340- 93.330	0.1160	1	0.498009	0.2177	0.1265
93.080- 93.070	0.1650	1	1.000009	0.4553	0.1950
95.000- 91.200	0.6460	1	0.498009	1.2121	0.7046
91.200- 89.000	3.5860	1	1.000009	9.8963	4.2386
89.000- 86.000	2.4900	1	1.000009	6.8716	2.9432
86.000- 84.000	0.8800	1	1.000009	2.4285	1.0402
83.500- 83.200	0.7530	1	1.000009	2.0781	0.8900
84.000- 81.000	1.3800	1	1.000009	3.8084	1.6312
81.000- 79.600	0.1820	1	1.000009	0.5023	0.2151
79.020- 79.010	0.4770	1	0.460009	0.8631	0.5169
78.780- 78.770	0.2780	1	0.460009	0.5030	0.3013
78.650- 78.640	0.1460	1	0.415009	0.2526	0.1570

λ (nm)	Reference Solar flux	K	C_λ	Solar flux solar max	solar min
				$(10^9$photons cm^{-2} s$^{-1})$	
78.040- 78.030	0.1310	2	0.022000	0.3512	0.1554
79.600- 78.000	0.1470	1	1.000009	0.4057	0.1738
77.050- 77.040	0.2420	2	0.022000	0.6489	0.2872
76.520- 76.510	0.2000	1	0.581009	0.4045	0.2211
76.035- 76.025	0.0930	1	0.473009	0.1704	0.1010
78.000- 76.000	0.1710	1	1.000009	0.4719	0.2021
76.000- 74.000	0.1720	1	1.000009	0.4747	0.2033
74.000- 73.200	0.0200	1	1.000009	0.0552	0.0236
70.340- 70.330	0.3920	1	0.415009	0.6783	0.4216
73.200- 70.000	0.1150	1	1.000009	0.3174	0.1359
68.580- 68.570	0.1010	1	0.523009	0.1940	0.1106
70.000- 66.500	0.0930	1	0.448009	0.1663	0.1006
66.500- 63.000	0.0880	1	0.415009	0.1523	0.0946
62.980- 62.490	1.5970	1	0.415009	2.7633	1.7176
60.980- 60.970	0.4500	2	0.028009	1.4132	0.5569
63.000- 60.000	0.0170	1	0.415009	0.0294	0.0183
59.970- 59.950	0.1900	1	0.415009	0.3288	0.2044
58.440- 58.430	1.5800	0*	$R_K(x)$=2.4420 $R_K(n)$=1.1500	3.8584	1.8170
55.440- 55.430	0.7990	1	0.460009	1.4458	0.8659
53.710- 53.700	0.1860	1	0.730009	0.4249	0.2107
50.795- 50.790	2.3920	1	0.415009	4.1388	2.5727
49.940- 49.930	0.0780	2	0.150000	0.9721	0.1773
60.000- 48.000	0.7050	1	0.830009	1.7347	0.8115
46.530- 46.520	0.3300	2	0.012600	0.6478	0.3653
48.000- 46.000	0.0560	1	0.830009	0.1378	0.0645
46.000- 43.500	0.1330	1	0.830009	0.3273	0.1531
43.500- 40.000	0.2690	1	0.481009	0.4967	0.2925
36.810- 36.800	0.7390	2	0.011040	1.3625	0.8082
36.090- 36.070	0.0180	2	1.000009	1.3936	0.1707
30.380- 30.370	6.0000	0*	$R_K(x)$=1.7755 $R_K(n)$=1.0839	10.6535	6.5035
40.000- 30.000	1.2960	1	0.481009	2.3930	1.4095
28.420- 28.410	0.1000	0*	$R_K(x)$=30.2186 $R_K(n)$= 4.1390	3.0219	0.4139
30.000- 28.000	0.1840	1	0.481009	0.3397	0.2001
27.430- 27.410	0.0500	2	0.150009	0.6232	0.1136
26.481- 26.479	0.0300	2	0.150009	0.3739	0.0682
28.000- 26.000	0.2980	2	0.150009	3.7142	0.6772
25.640- 25.630	0.2710	2	0.150009	3.3777	0.6159
26.000- 24.000	0.5970	2	0.150009	7.4409	1.3568
24.000- 22.000	0.3800	2	0.150009	4.7365	0.8636
22.000- 20.500	0.1000	2	0.150009	1.2464	0.2273
20.500- 19.000	0.4950	2	0.088109	3.8280	0.8650
19.000- 18.000	0.4500	2	0.088109	3.4800	0.7864
18.000- 16.500	0.9600	2	0.088109	7.4241	1.6776
16.500- 13.800	0.1380	2	0.088109	1.0672	0.2412
13.800- 10.300	0.0700	2	0.088109	0.5413	0.1223
10.300- 8.300	0.1540	2	0.088109	1.1909	0.2691
8.300- 6.200	0.1490	2	0.088109	1.1523	0.2604
6.200- 4.100	0.1070	2	0.088109	0.8275	0.1870
4.100- 3.100	0.0020	2	0.088109	0.0155	0.0035
3.100- 2.280	0.0070	2	0.088109	0.0541	0.0122
2.280- 1.500	0.0010	2	0.088109	0.0077	0.0017
1.500- 1.000	0.0010	2	0.088109	0.0077	0.0017